Electronic Supplementary Material (ESI) for Journal of Materials Chemistry A.
This journal is © The Royal Society of Chemistry 2024

# Supporting Information

## Graphene Nanoribbons/Ru as Efficient Cathodic Catalysts for High-Performance Rechargeable Li-$CO_2$ Batteries

*Xiaoling Ye,[a] Wencheng Liu,[a] Yan Lu,[b] Xiaoxiao Zheng,[a] Yijian Bi,[a] Min Zheng,[c] Lei Han,[a] Benqing Liu,[a] Yafei Ning,[a,d] Syed Hassan Mujtaba Jafri,[e,f] Xinyu Zhao,[*g] Shangming He [*h] Shilin Zhang[*c] and Hu Li[*a,d]*

[a] Shandong Technology Centre of Nanodevices and Integration, School of Integrated circuit, Shandong University, Jinan 250101, China.

[b] State Key Lab of High Performance Ceram and Superfine Microstructure, Shanghai Institute of Ceramics, Chinese Academy of Science, Shanghai 200050, P.R. China.

[c] School of Chemical Engineering, The University of Adelaide, Adelaide, SA 5000, Australia.

[d] Shenzhen Research Institute of Shandong University, Shenzhen, 518063, China.

[e] Department of Electrical Engineering, Mirpur University of Science and Technology, Mirpur Azad Jammu and Kashmir 10250, Pakistan.

[f] Department of Materials Science and Engineering Uppsala University, 75121 Uppsala, Sweden.

[g] Center for Orthopaedic Science and Translational Medicine, Department of Orthopaedics, Shanghai Tenth People's Hospital, School of Medicine, Tongji University, 301 Yanchang Road, Shanghai 200072, People's Republic of China.

[h] Shanghai Synchrotron Radiation Facility (SSRF), Shanghai Advanced Research Institute (SARI), and Shanghai Institute of Applied Physics, Chinese Academy of Sciences (CAS), 201204 Shanghai, P. R. China.

**Table S1.** Comparison of GNR Conductivity Before and After Annealing

| | Temperature (°C) | Resistivity (Ω·cm) | Conductivity (S $cm^{-1}$) |
|---|---|---|---|
| Before Annealing | 25 | 0.085 | 11.764 |
| After Annealing | 25 | 0.043 | 23 |

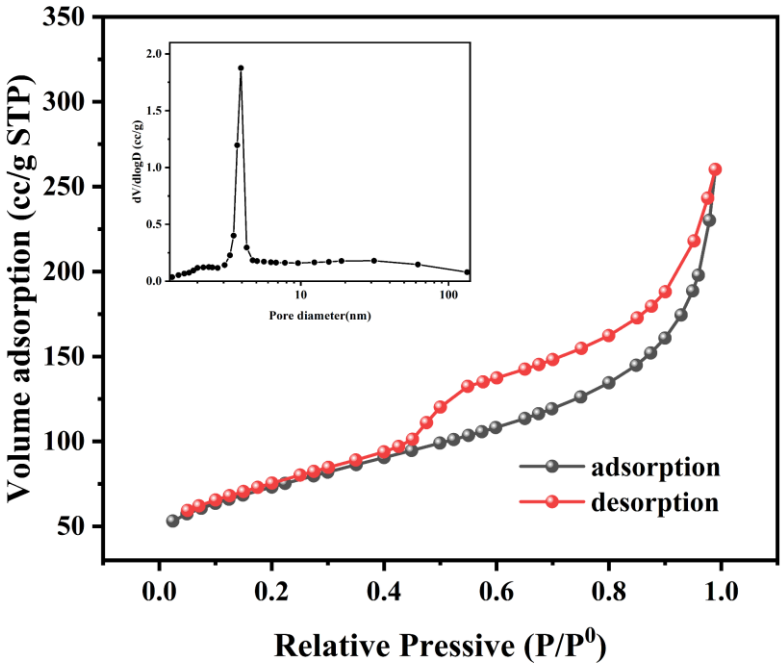


**Fig. S1** $N_2$ adsorption–desorption isotherms of GNR (inset is the pore size distribution).

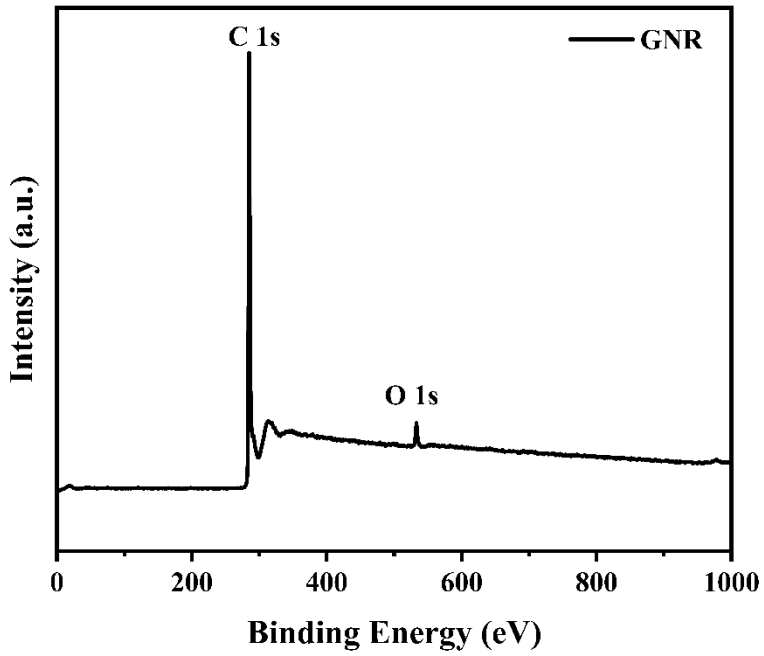


**Fig. S2** Full X-ray photoelectron spectroscopy of GNR.

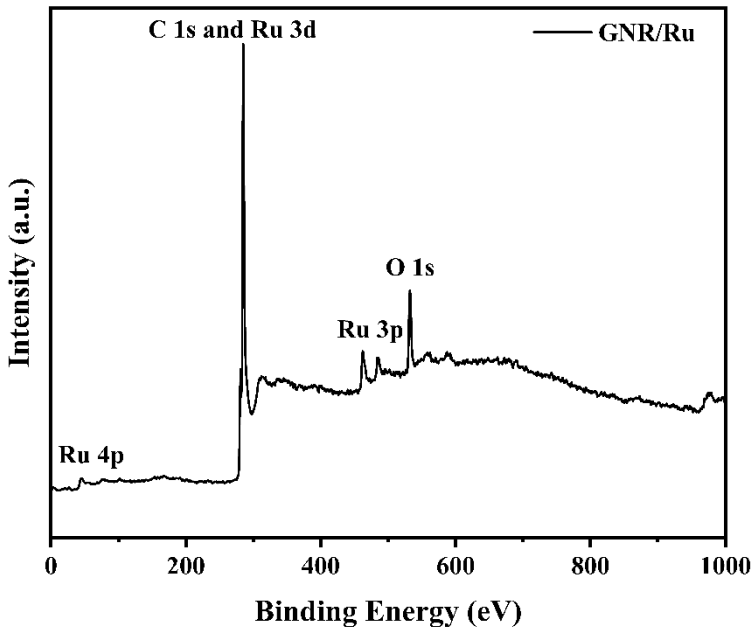


**Fig. S3** Full X-ray photoelectron spectroscopy of GNR/Ru.

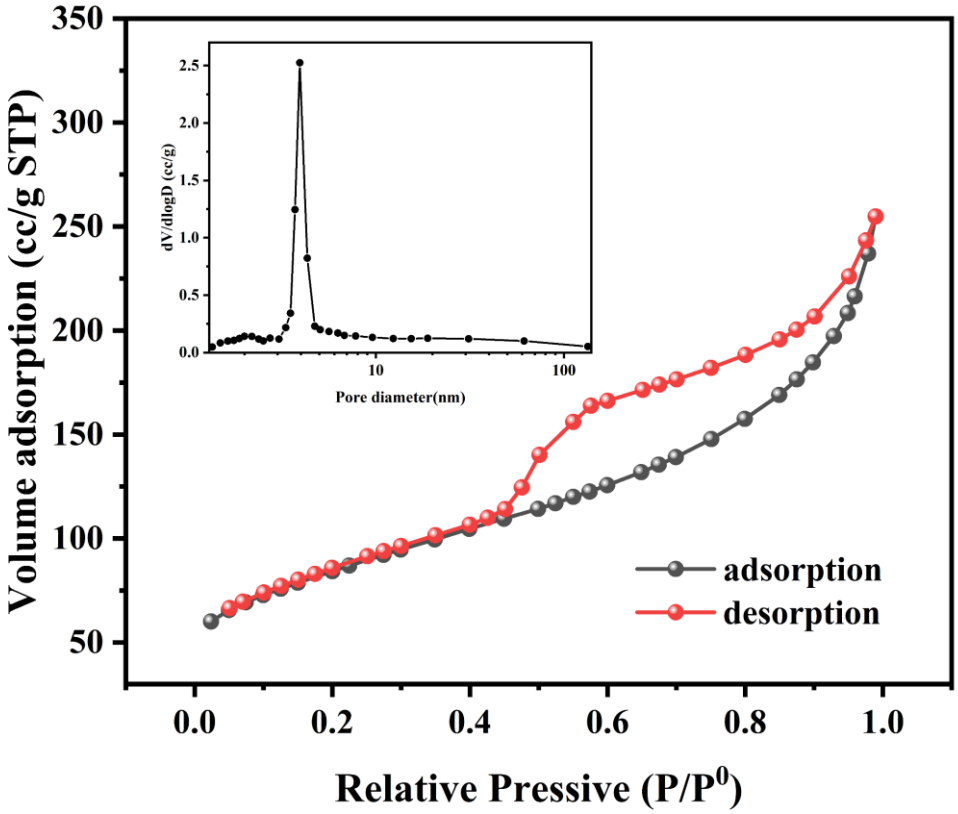


**Fig. S4** $N_2$ adsorption–desorption isotherms of GNR/Ru catalyst.

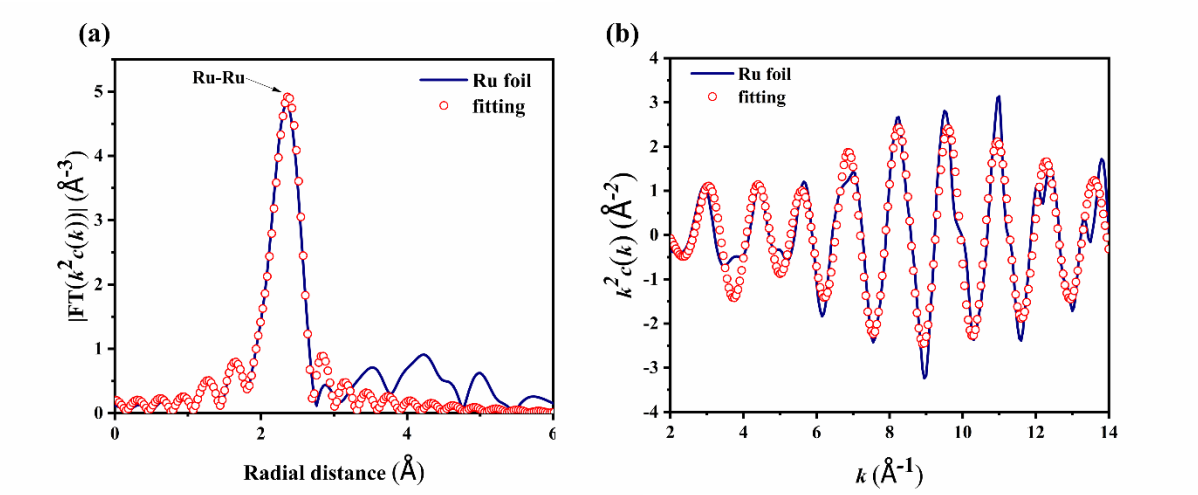


**Fig. S5** (a) Fitting of the magnitude of theFourier transform of the $k^2$-weighted EXAFS and (b) the corresponding $k^2$-weighted oscillation fitting curves (data-blue and fit-red) for Ru foil.

**Table S2.** EXAFS data fitting results of Samples.

| Sample | Path | *CN*[a] | *R*(Å)[b] | $\sigma^2$ (Å$^2$)[c] | $\Delta E_0$(eV)[d] | *R* factor |
|---|---|---|---|---|---|---|
| Ru K-edge ($S_0^2$=0.905) | | | | | | |
| Ru foil | Ru-Ru | 12* | 2.672±0.003 | 0.0041 | -5.0 | 0.0052 |
| GNR/Ru | Ru-C | 3.7±0.8 | 2.026±0.012 | 0.0015 | -12.25 | 0.0038 |
| | Ru-Ru | 5.1±0.4 | 2.668±0.003 | 0.0032 | -3.3 | |

[a]*CN*, coordination number; [b]*R*, the distance between absorber and backscatter atoms; [c]$\sigma^2$, the Debye Waller factor value; [d]$\Delta E_0$, inner potential correction to account for the difference in the inner potential between the sample and the reference compound; *R* factor indicates the goodness of the fit. $S_0^2$ was fixed to 0.905, according to the experimental EXAFS fit of Ru foil by fixing *CN* as the known crystallographic value. * This value was fixed during EXAFS fitting, based on the known structure of Ru. Fitting conditions: *k* range： 3.0 - 14.0; *R* range: 1.0 - 3.0; fitting space: R space; *k*-weight = 2. A reasonable range of EXAFS fitting parameters: 0.800 < $S_0^2$ < 1.000; *CN* > 0; $\sigma^2$ > 0 Å$^2$; $|\Delta E_0|$ < 15 eV; *R* factor < 0.02.

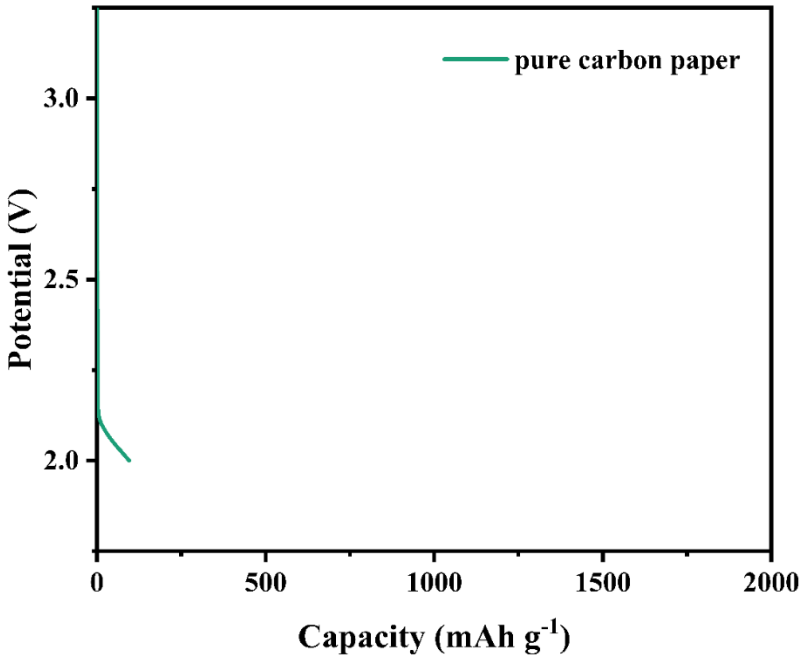


**Fig. S6** Full discharge profiles of catalyst-free carbon paper.

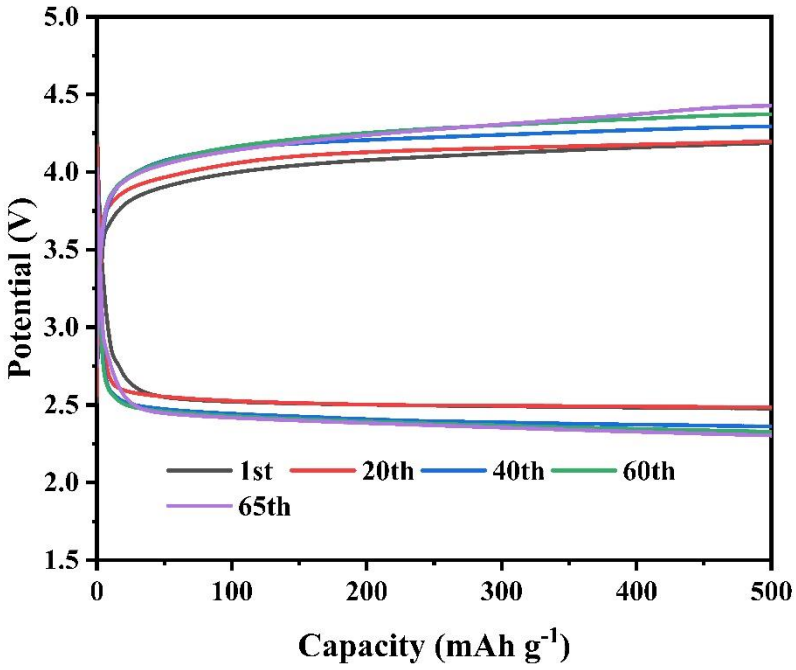


**Fig. S7** Selected discharge-charge curves for LCBs with the GNR cathode.

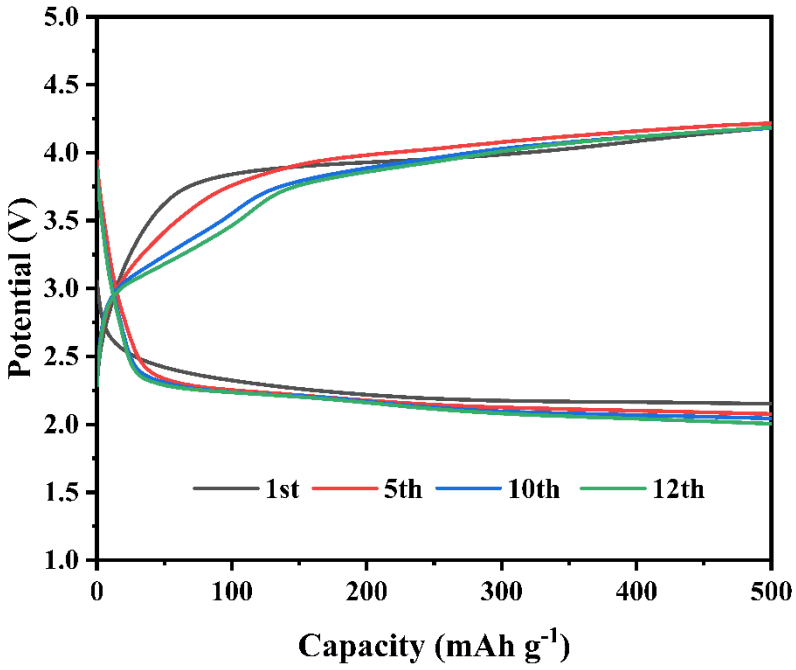


**Fig. S8** Selected discharge-charge curves for LCBs with the SWCNT cathodes.

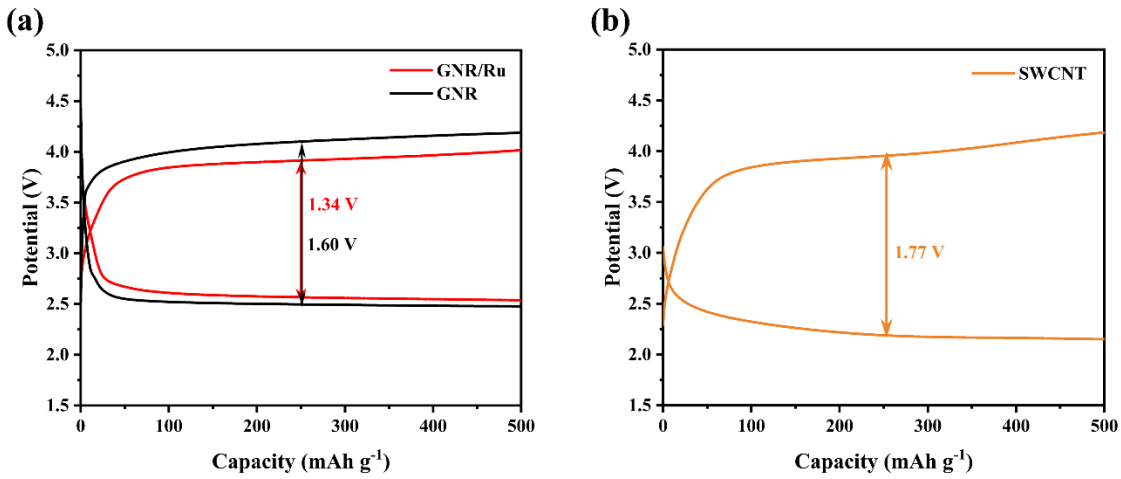


**Fig. S9** Cycling overpotentials of (a) GNR/Ru, GNR and (b) SWCNT.

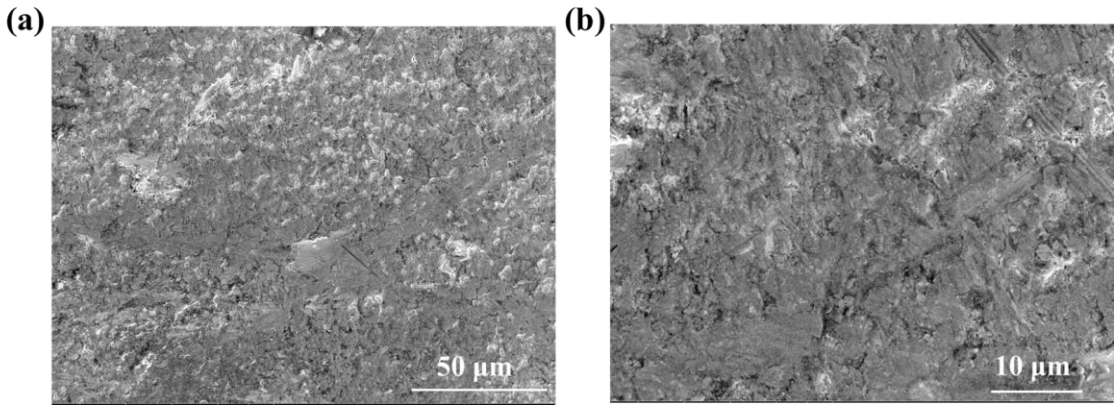


**Fig. S10.** SEM images of GNR/Ru cathode after long cycles.

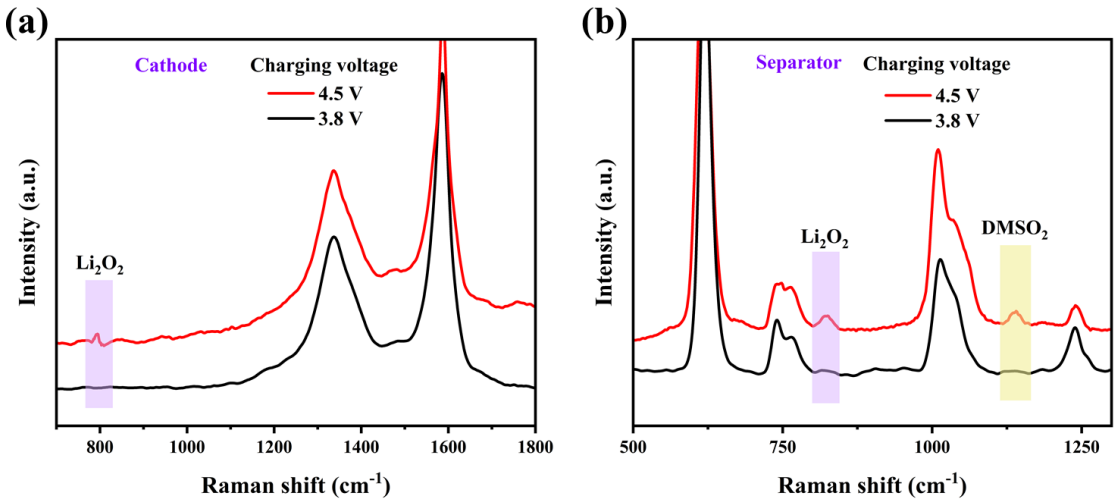


**Fig. S11** Raman spectra of (a) Cathode and (b) Separator at different charging voltage.

**Table S3.** The electrochemical performances comparisons of different LCBs reported in the literature.

| Cathodes Material | Discharge capacity (mAh $g^{-1}$) | Over-potential (V) | Battery operation time (h) | References |
|---|---|---|---|---|
| **GNR/Ru** | **11470 (100 mA $g^{-1}$)** | **1.34 (100 mA $g^{-1}$)** | **1240 (100 mA $g^{-1}$)** | **This work** |
| CNT/Ru | 4541 (100 mA $g^{-1}$) | 1.24 V (100 mA $g^{-1}$) | 450 (100 mA $g^{-1}$) | [1] |
| RuCo/CNFs | | 0.98 (100 mA $g^{-1}$) | 360 (500 mA $g^{-1}$) | [2] |
| Ru/ACNFs | | 1.35 (100 mA $g^{-1}$) | 1000 (100 mA $g^{-1}$) | [3] |
| CNT@$RuO_2$ | 2187 (50 mA $g^{-1}$) | ~1.4 (100 mA $g^{-1}$) | 1100 (50 mA $g^{-1}$) | [4] |
| NiPc-CN MDE | 18000 (200mA $g^{-1}$) | 1.4 (50 mA $g^{-1}$) | 1200 (50 mA $g^{-1}$) | [5] |
| $Co_{0.1}Ni_{0.9}O_x$/CNT | 5871.41 (100 mA $g^{-1}$) | 1.27 (100 mA $g^{-1}$) | 500 (100 mA $g^{-1}$) | [6] |
| Au/CNT | 6399 (100 mA $g^{-1}$) | 1.53 (100 mA $g^{-1}$) | 460 (200 mA $g^{-1}$) | [7] |
| MXene/GO | 18326 (100 mA $g^{-1}$) | 2.4 (100 mA $g^{-1}$) | 430 (100 mA $g^{-1}$) | [8] |
| $Ti_3C_2T_x$ MXene/CNT | | 1.38 (200 mA $g^{-1}$) | 1000 (200 mA $g^{-1}$) | [9] |
| Cu-NG | | 0.77 (100 mA $g^{-1}$) | 500 (200 mA $g^{-1}$) | [10] |
| NG/RGO | | 2.21 (500 mA $g^{-1}$) | 390 (500 mA $g^{-1}$) | [11] |
| CQD/hG | 12300 (50 mA $g^{-1}$) | 1.02 (100 mA $g^{-1}$) | 235 (1.0 A $g^{-1}$) | [12] |
| α-$MnO_2$/CNT | 7134.1 (50 mA $g^{-1}$) | 1.4 (100 mA $g^{-1}$) | 1000 (100 mA $g^{-1}$) | [13] |

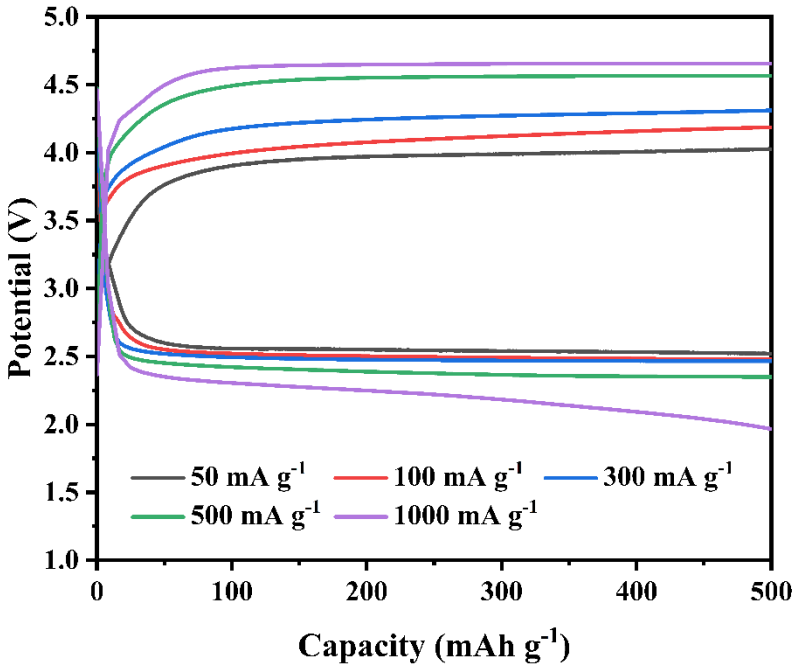


**Fig. S12** GNR cathodes at different current densities.

## References


1. K. V. Savunthari, C.-H. Chen, Y.-R. Chen, Z. Tong, K. Iputera, F.-M. Wang, C.-C. Hsu, D.-H. Wei, S.-F. Hu and R.-S. Liu, *ACS Applied Materials & Interfaces*, 2021, **13**, 44266-44273.
2. Y. Jin, F. Chen and J. Wang, *ACS Sustainable Chemistry & Engineering*, 2020, **8**, 2783-2792.
3. Y. Qiao, S. Xu, Y. Liu, J. Dai, H. Xie, Y. Yao, X. Mu, C. Chen, D. J. Kline, E. M. Hitz, B. Liu, J. Song, P. He, M. R. Zachariah and L. Hu, *Energy & Environmental Science*, 2019, **12**, 1100-1107.
4. S. Bie, M. Du, W. He, H. Zhang, Z. Yu, J. Liu, M. Liu, W. Yan, L. Zhou and Z. Zou, *ACS Applied Materials & Interfaces*, 2019, **11**, 5146-5151.
5. H. Zheng, H. Li, Z. Zhang, X. Wang, Z. Jiang, Y. Tang, J. Zhang, B. Emley, Y. Zhang, H. Zhou, Y. Yao and Y. Liang, *Small*, 2023, **19**, 2302768.
6. M. S. Choi, A. Nipane, B. S. Y. Kim, M. E. Ziffer, I. Datta, A. Borah, Y. Jung, B. Kim, D. Rhodes, A. Jindal, Z. A. Lamport, M. Lee, A. Zangiabadi, M. N. Nair, T. Taniguchi, K. Watanabe, I. Kymissis, A. N. Pasupathy, M. Lipson, X. Zhu, W. J. Yoo, J. Hone and J. T. Teherani, *Nature Electronics*, 2021, **4**, 731-739.
7. Y. Kong, H. Gong, L. Song, C. Jiang, T. Wang and J. He, *European Journal of Inorganic Chemistry*, 2021, **2021**, 590-596.
8. A. Bharti, G. Manna, P. Saha, G. Achutarao and A. J. Bhattacharyya, *The Journal of Physical Chemistry Letters*, 2022, **13**, 7380-7385.
9. Z. Hu, Y. Xie, D. Yu, Q. Liu, L. Zhou, K. Zhang, P. Li, F. Hu, L. Li, S. Chou and S. Peng, *ACS Nano*, 2021, **15**, 8407-8417.
10. Z. Zhang, Z. Zhang, P. Liu, Y. Xie, K. Cao and Z. Zhou, *Journal of Materials Chemistry A*, 2018, **6**, 3218-3223.
11. B. Chen, D. Wang, B. Zhang, X. Zhong, Y. Liu, J. Sheng, Q. Zhang, X. Zou, G. Zhou and H.-M. Cheng, *ACS Nano*, 2021, **15**, 9841-9850.
12. Y. Jin, C. Hu, Q. Dai, Y. Xiao, Y. Lin, J. W. Connell, F. Chen and L. Dai, *Advanced Functional Materials*, 2018, **28**, 1804630.
13. D. Lei, S. Ma, Y. Lu, Q. Liu and Z. Li, *Journal of Electronic Materials*, 2019, **48**, 4653-4659.